科技論文撰寫之
3C及五個章節

鄭木海講座教授 中興大學電機系/光電所

中興大學 2022年5月17日

概述(Overview)

一般科技論文撰寫需具備3C要件:清楚表達(Clear)、簡潔書寫(Concise)、正確文法(Correct)及五個章節：摘要(Abstract)、導論(Introduction)、方法(Method)、結果(Result)、及討論與結論(Discussion and Conclusion)。本文分享撰寫科技論文五個章節之技巧與範例，其中導論為最難撰寫，優良導論需具備一個Why(為什麼)及五個What(什麼意思)，由優良導論撰寫，可找出適合論文題目。本文並介紹期刊與會議論文撰寫之差異性及口頭與海報論文發表之差異。

國立中興大學
National ChungHsing University

科技論文撰寫大綱

一、摘要

二、導論

三、方法及結果

四、討論與結論

五、會議論文

六、總結

摘要(Abstract)

摘要可視為整體論文濃縮，也是整體論文簡短概述(Overview)，摘要內容要清楚敘述主要結論，非計畫簡介。優良摘要撰寫能使審稿者迅速對論文目的及結論有概略了解，並可使審稿者決定是否有必要詳讀整篇文章的內容，對論文有好的印象，提高論文被接受機會。**優良論文摘要撰寫應包含:目的、方法、結果、結論或結論之價值與意義。**撰寫結論之價值與意義可加值論文重要性，不宜忽略，結論之價值與意義可能為下列三點簡短概述之一：

學術貢獻－結論具學術價值(Academic innovation,學術創新性)

技術貢獻－結論具技術價值(Technical advance,技術進步性)

產業貢獻－結論具實用價值(Practical utilization,產業利用性)

摘要時態之撰寫

1.敘述摘要研究目的之撰寫可選擇二個方式:論文導向或研究導向

論文導向目的:論文目的為介紹自己研究活動，句子所提出資料不受時間影響，時態使用現在式，論文導向目的句子之開頭經常使用paper, report, thesis。

例 (1)This paper (report, thesis) presents data collected during a two-year survey of X.

(2) A numeric method is reported for solving the symmetric matrix eigenvalue problem.

研究導向目的:論文目的為介紹新技術或方法，或提出實驗結果，句子指已結束過去事情,時態使用過去式 ，研究導向目的句子之開頭經常使用study, investigation, experiment。

例 (1) In this study (investigation, experiment), a survey of X was conducted.

(2) Samples of neat solid trapped in excess ice were subjected to laser power of 10 W.

2.介紹摘要論文研究方法之時態，一般句子時態使用過去式

例:The multilayers graphene were grown by chemical vapor deposition on subtract.

3.說明摘要論文主要結果之時態 ，通常句子時態使用過去式

例:The scores of subjects who received a program were higher than the scores of the other two groups.

4.描述摘要結論或結論貢獻度，句子可使用現在式、或推測助動詞如 may, should, could

例 (1) The experimental results show the important devices in current optical components.

(2)The strong seasonal fluctuations of CO_2 may explain variations in base-cation concentrations.

範例1:Polarization Maintaining Fiber (極化保持光纖): PANDA Fiber(熊猫光纖)

熊猫

Slow axis →

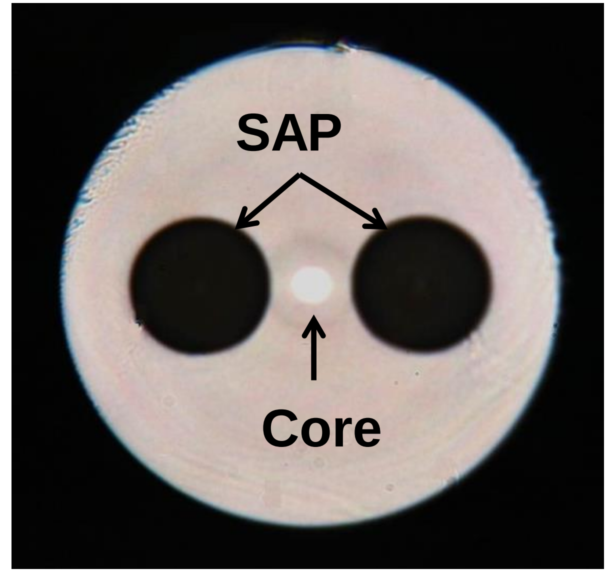

熊猫光纖 (Panda Fiber)

Fast axis ↑

極化保持光纖經常使用於光纖陀螺儀之衛星或飛彈導航應用

陀螺儀

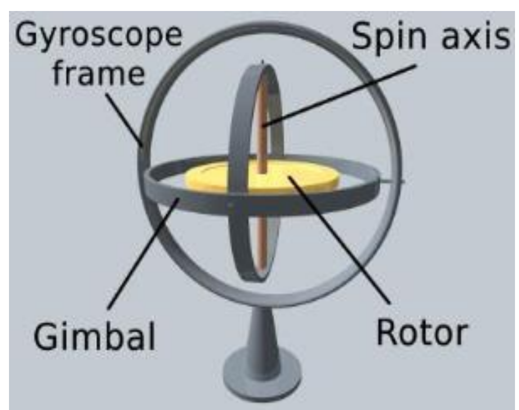

摘要撰寫範例(1)

A New Scheme of Oriented Hyperboloid Microlens for Passive Alignment Lasers to Polarization Maintaining Fibers

Wen-Hsuan Hsieh, Chun-Nien Liu, *Student Member, IEEE, Student Member, OSA*, Yi-Chung Huang, *Member, IEEE, Member, OSA*, Cheng-An Hsu, Shih-Chin Lei, Yi-Cheng Hsu, Ying-Chien Tsai, Che-Hsin Lin, Chin-Ping Yu, and **Wood-Hi Cheng**, *Fellow, IEEE, OSA*, J Lightwave Technol. 33, Oct. 4187 (2015).

Abstract—[1]A new scheme of oriented-hyperboloid microlens (OHM) with passive alignment to achieve high polarized extinction ratio (PER) is proposed and demonstrated for high efficiency coupling of high-power 980 nm pump lasers to polarization maintaining fibers (PMFs). [2]Using an automatic grinding machine and a charge-coupled-device to precisely control and attain the required minor radius of curvature 4–4.8 μm, offset within 0.7 μm, and axis orientation accuracy±1, [3]the OHM exhibited a high-average PER of 31.7 dB, and a high-average coupling efficiency of 83.4%. [3]For a 30 dB PER, the angular misalignment tolerance of the OHM was measured to be ±2°. [4]The unique advantage of the proposed OHM is passive alignment to achieve high PER by only aligning the OHM endface of the fast axis parallel to the axis of laser polarization. [4]This newly developed OHM with unique passive alignment to achieve high polarization is beneficial for the applications of laser/PMF modules where mode polarization and high coupling efficiency are required for use in high precision fiber optic gyroscopes as well as many low-cost and high-performance lightwave interconnection applications.

(1)目的(論文導向目的):時態現在式、(2)方法:時態過去式、(3)結果:時態過去式、(4)結論或結論貢獻度:時態現在式

範例2:石墨烯(Graphene)材料

石墨烯是一種由碳原子所組成六角型呈蜂巢晶格的平面二維薄膜(如圖)，2004年英國曼徹斯特大學物理學家安德烈·海姆和康斯坦丁·諾沃肖洛夫，成功在實驗從石墨中分離出石墨烯，兩人也因“在二維石墨烯材料的開創性實驗”，共同獲得2010年諾貝爾物理學獎。石墨烯目前是世上最薄卻也是最堅硬的納米材料，它幾乎是完全透明。

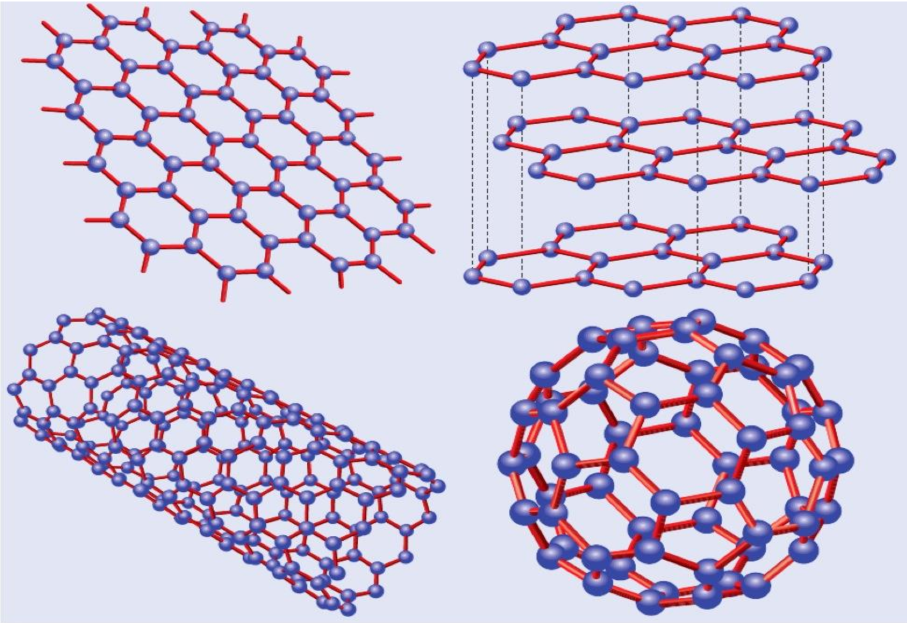

摘要撰寫範例(2)

Stable mode-locked fiber laser based on CVD fabricated graphene saturable absorber

Pi Ling Huang,[1] Shau-Ching Lin,[1] Chao-Yung Yeh,[2] Hsin-Hui Kuo[3], Shr-Hau Huang[1]
Gong-Ru Lin,[4] Lain-Jong Li,[5] Ching-Yuan Su,[5] and Wood-Hi Cheng[1,*]

30 January 2012, Vol. 20, No.3, 2460 OPTICS EXPRESS(論文被引用157次)

Abstract: [1]A stable mode-locked fiber laser (MLFL) employing multi-layer graphene as saturable absorber (SA) is presented. [2]The multi-layer graphene were grown by chemical vapor deposition (CVD) on Ni close to A-A stacking. [3]Linear absorbance spectrum of multi-layer graphene was observed without absorption peak from 400 to 2000 nm. [1]Optical nonlinearities of different atomic-layers (7-, 11-, 14-, and 21- layers) graphene based SA are investigated and compared. [3]The results found that the thicker 21-layer graphene based SA exhibited a smaller modulation depth (MD) value of 2.93% due to more available density of states in the band structure of multi-layer graphene and favored SA nonlinearity.[3]A stable MLFL of 21-layer graphene based SA showed a pulsewidth of 432.47 fs, a bandwidth of 6.16 nm, and a time-bandwidth product (TBP) of 0.323 at fundamental soliton-like operation. [4]This study demonstrates that the atomic-layer structure of graphene from CVD process may provide a reliable graphene based SA for stable soliton-like pulse formation of the MLFL.

(1)目的(論文導向目的):時態現在式、(2)方法:時態過去式、(3)結果:時態過去式、(4)結論或結論貢獻度:時態現在式(或推測助動詞如 may, should, could)

科技論文撰寫大綱

一、摘要

二、導論

三、方法及結果

四、討論與結論

五、會議論文

六、總結

導論(Introduction)

導論撰寫有五個主要功能:1.說明研究動機、2.文獻回顧、3.敘述研究方法、4.敘述研究目的、及5.陳述預期目標。一篇公認優良科技學術論文導論的撰寫需具備一個Why(為什麼)及五個What(什麼意思) 。

1.Why is the topic of interest?研究動機:主題引起讀者興趣之原因及重要

1.What is the background on the previous solutions?文獻回顧:過去解決問題的背景

2.What is the background on potential solutions?研究方法:提出解決問題可能的方案

3.What will be presented in this paper?研究目的:提出問題解決的目的

4.What is attempted in the present effort?預期目標:擬達成目標及價值

5.What is organized in this paper?論文組織架構:假如論文為短文(Letter),本項目可選擇從缺

由優良導論撰寫,可找出適合科技論文之研究題目。

導論功能與時態之撰寫

1. 研究動機:說明主題引起讀者興趣的原因及重要性,資料撰寫動機先舊後新,時態使用現在式。
2. 文獻回顧:敘述過去解決問題的背景,一般句子之時態使用現在式,或現在完成式,或過去式。
3. 研究方法:提出解決問題可能方案,一般句子之時態使用現在式。
4. 研究目的:提出問題解決之目的,敘述研究目的或主要研究活動,文章可選擇論文導向(現在式時態)或研究導向(過去式時態)。
5. 預期目標:擬達成目標及價值,描述結論建議或貢獻度,作者可使用現在式時態、或使用推測助動詞如may, should, could。
6. 論文組織架構:描述論文組織架構,一般句子之時態使用現在式。

   例:The organization of this paper is as follows. Section 2 presents the basic analysis. In section 3, experimental results are presented. The conclusion of the paper is stated in the last section.

導論撰寫範例 (1)

I. INTRODUCTION (JLT)

[1]POLARIZATION maintaining fibers (PMFs) with a double refractive index are single-mode fibers which exhibit good maintenance of linearly polarized light [1]. [1]The PMFs are used in special applications required for preserving polarization properties, such as fiber optic sensing, interferometry, and high- standard lightwave interconnection applications. [1]They are also commonly used in fiber optic gyroscopes for the connection between a high-power 980 nm pump lasers coupled to a modulator via PMFs, since the modulator requires polarized light as input source. [1]The PMFs are called polarization preserving because they allow for the preservation and control of the mode polarization state. [1]Therefore, an accurate alignment between pump lasers and PMFs to achieve high coupling efficiency is important to the development of high-performance pump laser modules.

[2]To achieve a high-coupling pump laser module, a common approach is fabricating the tip of single-mode fiber (SMF) as an asymmetric microlens for direct coupling. [2]Several asymmetric microlens structures for coupling to high-power 980 nm pump laser diodes have been demonstrated, such as up-tapered wedge- shaped fibers [2], asymmetric hyperbolic fiber microlenses [3]– [5], anamorphic lenses [6], wedge-shaped fibers [7]–[9], QPSM [10], CWSM [11], AECSM [12], DVCM [13], and HM [14]. [3]Despite numerous studies of fiber microlenses for efficient coupling [2]–[14], only limited information is available regarding the accurate positioning necessary for controlling the state of mode polarization for PMFs used in high-performance laser modules.

1.研究動機:現在式, 2.文獻回顧:現在式,現在完成式或過去式, 3.提出研究方法:現在式

導論撰寫範例 (1)-Continue

[4]In this study, a new scheme of oriented-hyperboloid-microlens (OHM) employing automatic grinding and accurate positioning to achieve both high-average coupling and polarized extinction ratio (PER) for high-power 980 nm pump lasers coupled to PMFs is proposed. The PMF exhibits the circular stress-applying parts (SAP) and is often referred to as the panda fiber, as shown in Fig. 1. [5]Using an automatic grinding machine and a charge-coupled-device (CCD) to precisely control and attain the required minor radius of curvature, small offset, and axis orientation, the OHMs can achieve both high-average coupling efficiency and PER. [5]The advantage of orientation-dependent OHMs is that the OHM endface of the fast axis can be visually observed and then passively aligned to the axis of the laser polarization direction. [5]This is in contrast to other conventional lasers coupled to PMFs [3], which may require complicated and active alignment to control the state of mode polarization. [5]This study demonstrates that the unique OHM structure employing automatic grinding and accurate positioning techniques enables passive alignment to achieve high PER for lasers coupling into PMFs. [5]Therefore, the proposed OHM may be suitable for use in high-precision and high-performance fiber-optic gyroscope systems and other lightwave interconnection applications.

[6]The rest of this paper is organized as follows. Section II describes the fabrication of OHMs. The measurements and results are presented in Section III. A discussion and brief summary are given in Section IV.

4.研究目的(論文導向目的):現在式, 5.預期目標:現在式, 6.論文組織架構:現在式

導論撰寫範例(2)

1. Introduction (OE)

[1]Ultrafast lasers possess several applications, such as optical fiber communications, ultrafast probing, nonlinear microscopy, optical coherent tomography, and frequency comb generation [1-2]. [1]A passively mode-locked erbium-doped fiber laser (MLEDFL) is able to generate pulses ranging from picosecond (ps) to femtosecond (fs). [1]The pulse producing mechanism is initiated from noise filtering by saturable absorber (SA) with nonlinear absorption properties [3]. [1]The SA widely used in passive mode-locked lasers is semiconductor saturable absorber mirror (SESAM). [1]However, the drawbacks of SESAM are cost-ineffective and a time-consuming fabricated process. [2]Recently, single-wall carbon nanotubes (SWCNTs) of 1D and graphene of 2D carbon allotrope have been noticed due to their large optical nonlinearity and low saturation intensity [4-7]. [2]The first passive mode-locked fiber laser (MLFL) based on SWCNT-SA was reported by S. Y. Set et al. in 2003 [8]. [2]Recently, the atomic layer graphene as SA for ultrafast pulsed lasers were also demonstrated by Q. Bao et al. [9-12]. [2]Graphene has excellent optical properties, such as optically visualized, high transparency, and linear absorption. [2]It also has ultra-fast relaxation time and the SA is not limited by band gap because of its point band gap structure. [1]Therefore, graphene can be used as fast SA with wide spectral operated range [13-16]. [2]However, mono-atomic layer graphene have relatively high nonlinearity that makes a laser cavity not easy to form a stable soliton pulse [9]. [2]In our nonlinear optical transmission experiments, we recognized that in addition to saturable absorption, the inverse saturation absorption (ISA) could also be formed at a higher intensity level. [2]The ISA could be caused by two photon absorption (TPA) which was similar to the phenomena reported in the SESAM SA [17]. [2]The ISA from a thinner layer graphene could destroy the stability of the mode locked

1.**研究動機:現在式, 2.文獻回顧:用現在式,現在完成式過去式,**

導論撰寫範例(2)-Continue

pulse formation. [2]Consequently, a thicker layer of graphene with less nonlinearity was identified as the mode locker to reduce the TPA and suppress the ISA. [2]Furthermore, atomic-layer graphene showed high nonlinear absorption which implied high nonlinear dispersion from Kramers-Kronig relationship. [2]Total dispersion was contributed from all the optical elements in the cavity including linear and nonlinear dispersion [9, 18-19]. [2]The nonlinear dispersion, such as self phase modulation (SPM) was contributed from SMF and high-order dispersion of graphene. [2]The total nonlinear dispersion inside the laser cavity could be compensated by anomalous linear dispersion from SMF to generate stable soliton pulses [9].

[3]In this study, optical nonlinearities of different atomic-layers (7-, 11-, 14-, and 21- layers) graphene based SA are investigated and compared. [4]It was found that the thicker 21-layer graphene based SA exhibited a small MD value of 2.93%. [4]Compared with the thinner 7-, 11-, and 14- layers, the results showed that a better stable MLFL with the thicker 21-layer graphene based SA exhibited a pulsewidth of 432.47 fs, a bandwidth of 6.16 nm, and a time-bandwidth product (TBP) of 0.323 at fundamental soliton-like operation. [5]This study demonstrates that the atomic-layer structure of graphene from CVD process may provide a reliable graphene based SA for stable soliton-like pulse formation of the MLFL.

2.文獻回顧:現在式,現在完成式或過去式, 3.提出研究方法:現在式, 4.研究目的(研究導向目的):過去式, 5.預期目標:現在式, 6.論文組織架構:論文為短文(Letter)，本項目從缺

科技論文撰寫大綱

一、摘要

二、導論

三、方法及結果

四、討論與結論

五、會議論文

六、總結

方法(Method)

優良科技學術論文撰寫的方法，應包括可重復(Repeatable)的實驗及清楚與簡潔(Clear and Concise)的圖表與統計分析，因此研究方法章節的撰寫，作者需詳細說明如何(How)進行研究工作及獲得研究結果的方法。一篇優良科技論文方法的撰寫，可能包括以下四點：(範例1、範例2)

1.材料

2. 實驗(架構、步驟、製程)

3.量測

4.圖表或 統計分析

研究方法時態之撰寫

1.材料:描述研究方法所使用材料，若材料為一般不受時間影響事實，句子時態使用現在式。例: A twin-lens reflex camera is actually a combination of two separate camera boxes.

若材料內容為特定過去事件，則句子時態使用過去式。例: The samples were held by special Al tabs covered with sandpaper.

2.實驗(架構、步驟、製程):陳述研究實驗過程，包括架構、步驟、製程，都是作者過去研究活動，這些說明句子時態使用過去式。

例: (1) The experiment was conducted at a large university in the Midwest.

(2) The 72 subjects were randomly divided into three groups.

3. 量測、圖表分析、或統計分析:在描述結果之前，經常出現介紹研究方法之句子，例如介紹量測、圖表或統計分析，這些句子內容不受時間影響之事實，因此句子時態使用簡單的現在式。

例: (1) The variation in the temperature of the samples over time is shown in Figure 1.

(2) Figure 1 shows the variation in the temperature of samples over time.

科技論文撰寫大綱

一、摘要

二、導論

三、方法及結果

四、討論與結論

五、會議論文

六、總結

結果(Result)

科技論文於結果章節撰寫，需要陳述主要研究結果，至於詳細的結果則可使用圖表列出。圖表的內容應盡量清楚與簡潔，使讀者不需看完文章說明，就能容易領會圖表中的訊息，因此圖表的標題必須清楚。一篇優良科技論文結果的撰寫，應包括以下三點：(範例1、範例2)

1. 研究結果介紹
2. 主要結果描述
3. 圖表或統計分析結果

結果時態之撰寫

在描述結果之前，經常出現介紹研究結果之句子，例如介紹圖表或統計分析，這些句子內容不受時間影響之事實，因此句子時態使用簡單的現在式。

例: Figure 1 shows the linearly polarized distribution of light through the OHM and cleaved end PMF.

說明論文主要結果,通常句子之時態使用過去式。

例:The scores of subjects who received a program were higher than the scores of the other two groups.

科技論文撰寫大綱

一、摘要

二、導論

三、研究方法及結果

四、討論與結論

五、會議論文

六、總結

討論撰寫(Discussion)

科技論文討論章節之目的在於探討研究結果之蘊涵，使讀者了解作者研究結果之重要性及未來展望(Future work)，典型討論章節可包括下列四項目：

1. 結果概述(研究成果是否跟其他結果一致性)
2. 推論(研究成果能支持較廣泛推論或結論)
3. 研究方法或結果的限制(非必要選項)
4. 建議新的研究題目(非必要選項)

結論撰寫(Conclusion)

技科論文於結論章節之目的在於敘述主要結論，而不在於概述(Overview)論文的所有內容，使讀者了解作者研究結果之重要性及可能貢獻度，一般結論章節的撰寫，應包括以下二點：

1. 陳述最重要的研究結果　2. 指出結論的貢獻度

結論的貢獻度可能為:

學術貢獻－所獲結論具學術價值(Academic innovation,學術創新性)

技術貢獻－所獲結論具技術價值(Technical advance,技術進步性)

產業貢獻－所獲結論具實用價值(Practical utilization,產業利用性)

國立中興大學 National ChungHsing University

討論與結論撰寫範例(1)

討論:1. 結果概述, 2.推論, 3.限制, 4.建議新的研究題目

結論:1. 陳述最重要的研究結果,2. 指出結論的貢獻度

DISCUSSION AND CONCLUSION (JLT)

[1]In summary, a novel OHM employing automatic grinding and CCD accurate positioning for passive alignment, which can achieve high PER and efficient coupling of high-power 980 nm pump lasers into PMFs, has been proposed and demonstrated. [1]Results showed that the OHMs enabled precisely control and attain the required minor radius of curvature at 4–4.8 μm, offset within 0.7 μm, and axis orientation $\pm 1^{\circ}$, for achieving a high- average coupling efficiency of 83.4% and a high-average PER of 31.7 dB from lasers coupling into PMFs. [1]The fabricated axis orientation accuracy of the OHM was $\pm 1^{\circ}$, which was less than the alignment tolerance of $\pm 2^{\circ}$ required to achieve a high PER of 30 dB. [2]This indicates that the OHM endface of the fast axis can be visually observed and passively aligned to the axis of the laser polarization direction. [2]The unique advantage of OHM is that OHM can be easily used for passive alignment to achieve high polarization of laser. [2]This is in contrast to other conventional lasers coupled to PMFs, which may require complicated and active alignment to control the state of mode polarization. [2]In addition, the proposed OHM can be also applied to other types of laser diodes, such as high-power 1480 nm laser diode, by suitable designing of the minor radius of curvature of the OHM to match the laser mode.

[4]The practical packaging of the OHM is based on the butterfly- type laser module in reference [17]. [4]Before the gripper clamping the OHM fiber ferrule, the ferrule should be adjusted such that the fast axis of the OHM, as shown in Fig. 3, is in the horizontal direction. [4]All the other packaging procedures are similar to that of the butterfly-type laser modules [17]. [2]This novel design, fully automatic fabrication, and excellent performance of the OHM makes the proposed OHMs potentially attractive for uses in high precision fiber optic gyroscopes as well as many high-performance and low-cost lightwave interconnection applications.

討論與結論撰寫範例(2)

結論:1. 陳述最重要的研究結果,2. 指出結論的貢獻度

4. Conclusion (OE)

[1]In summary, the 7-, 11-, 14- and 21- layers graphene based SA with different SMF fiber lengths for the generation of ultrafast laser pulse were comprehensively studied and compared. [2]It was found that the thinner 7-, 11- and 14- layers of graphene based SA had difficulty in forming a stable soliton-like pulse unless extra SMFs were added. [2]The reason was the thinner layer graphene samples exhibited relatively high MD with ISA made it difficult for a laser cavity to form a stable soliton pulse and needed additional length of SMF to compensate the dispersion. [2]In comparison with the thicker 21-layer graphene as SA, a stable mode locking pulse train was easier to establish. [2]This might be due to more available density of states in the band structure of stacking-layer graphene than the thinner layer and favored nonlinear optics control of graphene inside the laser cavity.

[1]The results showed that the optical nonlinearity of the thick 21-layer graphene based SA exhibited a smaller MD value of 2.93% and a higher saturation intensity of 53.25 MW/cm^2. [1]A stable MLFL of 21-layer graphene based SA showed a pulsewidth of 432.47 fs, a bandwidth of 6.16 nm, and a TBP of 0.323 at fundamental soliton-like operation. [2]This study demonstrated that the atomic-layer structure of graphene from a CVD process provided a reliable graphene based SA for stable soliton-like pulse formation of the MLFL.

科技論文撰寫大綱

一、摘要

二、導論

三、研究方法及結果

四、討論與結論

五、會議論文

六、總結

投稿期刊與會議論文撰寫之差異性

期刊論文：倒金字塔架構 ∇　會議論文：金字塔架構 Δ

期刊論文	會議論文
簡介	重要結果或發現
研究方法	簡介
重要結果或發現	究研方法
結果及討論	結果及討論

發表同一篇文章於研討會與期刊論文之可能性

1.發表同一篇研討會論文與期刊論文之投稿期刊論文時間選擇:三種時間可能之選擇

(1)投稿研討會後

(2)研討會論文被接受後

(3)發表研討會論文後

2.同一篇研討會論文與期刊論文內容之區別:投稿期刊論文之內容，必需有40 - 60%不同於研討會會議論文之內容。

發表口頭及海報論文之差異性

發表會議論文方式可選擇口頭報告(Oral)或張貼海報(Poster):

1.一般發表於重要國際會議之口頭報告論文接受率低於海報論文。

2.研究生出席國際會議，申請科技部補助，通常發表海報論文補助之重要性低於發表口頭論文。

3.英文程度不流利的作者可選擇海報論文發表。

發表海報論文之秘訣(1)

1.以海報呈現論文，需以簡明扼要的形式來呈現研究要點，以利觀眾快速了解並吸收論文內容。雖然論文以海報呈現的格式不同於期刊論文，但是概念大致相同，依序分成「前言」、「研究方法」、「研究結果」、「結論」等段落。結論是最關鍵的段落，必須連貫開場白。

2.海報設計不能太複雜，字體不能太小，必須讓觀眾能藉由近距離能閱讀海報。

發表海報論文之秘訣(2)

1. 標題、作者、作者服務單位：這個段落通常出現在海報最上方，論文標題務必切題扼要，最好能用幾個字描述主要研究發現。

2. 簡短介紹與研究主題最相關前人文獻：海報上前言通常只是淺談前人研究，或是介紹論文主體的一小部分，將前人發現的議題直接引入研究主題，讓觀眾兩分鐘內便能讀完這個段落。

3. 簡明描述研究中的主要方法：研究方法的段落必須介紹研究設計、研究方法與研究過程。如果牽涉到複雜的儀器或實驗設計，最好使用圖表說明。

4. 研究結果：這是海報最重要的段落，通常這部分會以圖表呈現，佐以文字解釋。圖表越大越好，比起內文更易於閱讀，使觀眾不必回顧海報前面的段落，便能理解研究結果。

5. 精簡討論或結論：結論通常只是一個短小的篇幅，但如果必須針對研究潛在問題加以討論，觀眾最好在兩分鐘內便能看完這個段落。

6. 參考文獻（非必要選項）：許多人會選擇刪除參考文獻，以增加海報上空間。如果你會提供更詳盡的講義，也可考慮將文獻列在上頭。

科技論文撰寫大綱

一、摘要

二、導論

三、研究方法及結果

四、討論與結論

五、會議論文

六、總結

總結1 - 優良科技學術論文內涵

一篇優良科技學術論文內涵，需包含以下七點：

1. 有科學原創性或技術進步性或產業利用性
2. 清楚(Clear)的文字表達
3. 簡潔(Concise)的文字技巧
4. 正確(Correct)的文法
5. 簡單(Simple)的統計分析法
6. 清楚與簡潔(Clear and Concise)的圖表表示
7. 完整(Integrity)的參考文獻

總結2 - 完整科技學術論文大綱

一篇完整的科技學術論文撰寫大綱，可包含以下七點：

(一) 摘要（Abstract）

研究主題、方法、結果、結論或貢獻度

(二)導論（Introduction）

背景、文獻回顧、方法、目的、預期成果、組織架構(選項）

(三) 研究方法（Method）

材料、架構、製程、量測、圖表分析、統計分析

(四) 結果（Result）

研究結果介紹、主要結果描述、圖表或統計分析結果

(五) 討論（Discussion)

結果概述、推論、研究方法或結果限制、建議新研究題目

(六) 結論（Conclusion）

簡潔最重要研究結果、結論或貢獻度

(七) 參考文獻（References）

總結3 - 結論陳述方式

論文結論於摘要、導論及結論章節陳述方式之差異：由於摘要、導論及結論章節撰寫各有不同功能，適合在其中一個章節句子，很可能在另外兩個章節中並不適用。因此，陳述結論時，不宜於摘要、導論及結論使用重複一模一樣的句子。因此，結論陳述方式之差異為:

	結論陳述方式之差異
摘要	結論宜簡略敘述:全篇論文的濃縮，使讀者對論文立即全面概略了解，結論簡略即可。
導論	以試探方式指出研究預期目標或結論：導論章節說明研究動機、敘述研究目的及陳述預期目標，以試探方式(may, should or could)指出研究預期目標或結論，而非詳述結論。
結論	詳述論文重要研究結果、指出結論的貢獻度。

結論陳述方式於摘要範例(1)

A New Scheme of Oriented Hyperboloid Microlens for Passive Alignment Lasers to Polarization Maintaining Fibers

摘要:結論宜簡略敘述

Abstract—[1]A new scheme of oriented-hyperboloid microlens (OHM) with passive alignment to achieve high polarized extinction ratio (PER) is proposed and demonstrated high efficiency coupling of high-power 980 nm pump lasers to polarization maintaining fibers (PMFs). [2]Using an automatic grinding machine and a charge-coupled-device to precisely control and attain the required minor radius of curvature 4–4.8 μm, offset within 0.7 μm, and axis orientation accuracy±1°, [3]the OHM exhibited a high-average PER of 31.7 dB, and a high-average coupling efficiency of 83.4%. [3]For a 30 dB PER, the angular misalignment tolerance of the OHM was measured to be ±2°. [4]The unique advantage of the proposed OHM is passive alignment to achieve high PER by only aligning the OHM endface of the fast axis parallel to the axis of laser polarization. [5]This newly developed OHM with unique passive alignment to achieve high polarization is beneficial for the applications of laser/PMF modules where mode polarization and high coupling efficiency are required for use in high precision fiber optic gyroscopes as well as many low-cost and high-performance lightwave interconnection applications.

(1)目的、(2)方法、(3)結果、(4)結論、(5)結論建議或貢獻度

結論陳述方式於導論範例(2)

導論:以試探方式指出研究預期目標或結論 I. INTRODUCTION

1POLARIZATION maintaining fibers (PMFs) with a double refractive index are single-mode fibers which exhibit good maintenance of linearly polarized light [1]. The PMFs are used in special applications required for preserving polarization properties, such as fiber optic sensing, interferometry, and high- standard lightwave interconnection applications. They are also commonly used in fiber optic gyroscopes for the connection be- tween a high-power 980 nm pump lasers coupled to a modulator via PMFs, since the modulator requires polarized light as input source. The PMFs are called polarization preserving because they allow for the preservation and control of the mode polar-ization state. 1Therefore, an accurate alignment between pump lasers and PMFs to achieve high coupling efficiency is important to the development of high-performance pump laser modules.

2To achieve a high-coupling pump laser module, a common approach is fabricating the tip of single-mode fiber (SMF) as an asymmetric microlens for direct coupling. Several asymmetric microlens structures for coupling to high-power 980 nm pump laser diodes have been demonstrated, such as up-tapered wedge- shaped fibers [2], asymmetric hyperbolic fiber microlenses [3]– [5], anamorphic lenses [6], wedge-shaped fibers [7]–[9], QPSM [10], CWSM [11], AECSM [12], DVCM [13], and HM [14]. 3Despite numerous studies of fiber microlenses for efficient coupling [2]–[14], only limited information is available regarding the accurate positioning necessary for controlling the state of mode polarization for PMFs used in high-performance laser modules.

4In this study, a new scheme of oriented-hyperboloid-microlens (OHM) employing automatic grinding and accurate positioning to achieve both high-average coupling and polarized extinction ratio (PER) for high-power 980 nm pump lasers coupled to PMF is proposed. The PMF exhibits the circular stress-applying parts (SAP) and is often referred to as the panda fiber, as shown in Fig. 1. **3Using an automatic grinding machine and a charge-coupled-device (CCD) to precisely control and attain the required minor radius of curvature, small offset, and axis orientation, the OHMs can achieve both high-average coupling efficiency and PER. 5The advantage of orientation-dependent OHMs is that the OHM endface of the fast axis can be visually observed and then passively aligned to the axis of the laser polarization direction. 5This is in contrast to other conventional lasers coupled to PMFs [3], which may require complicated and active alignment to control the state of mode polarization. 5This study demonstrates that the unique OHM structure employing automatic grinding and accurate positioning techniques enables passive alignment to achieve high PER for lasers coupling into PMFs. 5Therefore, the proposed OHM may be suitable for use in high-precision and high-performance fiber-optic gyroscope systems and other lightwave interconnection applications.**

6The rest of this paper is organized as follows. Section II de- scribes the fabrication of OHMs. The measurements and results are presented in Section III. A discussion and brief summary are given in Section IV.

1.研究動機, 2.文獻回顧, 3.提出研究方法, 4.研究目的, 5.預期目標, 6.論文組織架構

結論陳述方式於結論範例(3)

結論: 詳述論文重要研究結果、指出結論的貢獻度

DISCUSSION AND CONCLUSION

[1]In summary, a novel OHM employing automatic grinding and CCD accurate positioning for passive alignment, which can achieve high PER and efficient coupling of high-power 980 nm pump lasers into PMFs, has been proposed and demonstrated. [1]Results showed that the OHMs enabled precisely control and attain the required minor radius of curvature at 4–4.8 μm, offset within 0.7 μm, and axis orientation ±1˚, for achieving a high-average coupling efficiency of 83.4% and a high-average PER of 31.7 dB from lasers coupling into PMFs. [1]The fabricated axis orientation accuracy of the OHM was ±1˚, which was less than the alignment tolerance of ±2˚ required to achieve a high PER of 30 dB. [2]This indicates that the OHM endface of the fast axis can be visually observed and passively aligned to the axis of the laser polarization direction. [2]The unique advantage of OHM is that OHM can be easily used for passive alignment to achieve high polarization of laser. This is in contrast to other conventional lasers coupled to PMFs, which may require complicated and active alignment to control the state of mode polarization. [2]In addition, the proposed OHM can be also applied to other types of laser diodes, such as high-power 1480 nm laser diode, by suitable designing of the minor radius of curvature of the OHM to match the laser mode.

[1]The practical packaging of the OHM is based on the butterfly- type laser module in reference [17]. [1]Before the gripper clamping the OHM fiber ferrule, the ferrule should be adjusted such that the fast axis of the OHM, as shown in Fig. 3, is in the horizontal direction. [2]All the other packaging procedures are similar to that of the butterfly-type laser modules [17]. [2]This novel design, fully automatic fabrication, and excellent performance of the OHM makes the proposed OHMs potentially attractive for uses in high precision fiber optic gyroscopes as well as many high-performance and low-cost lightwave interconnection applications.

討論:1. 結果概述, 2.推論, 3.限制, 4.建議新的研究題目

結論:1. 陳述最重要的研究結果,2. 指出結論的貢獻度

總結 4 -回覆重大修改 (Major revise)評論之技巧

收到審稿者與編輯於審查評論中提出要求重大修改(Major revise)意見,且有些重大意見困難回覆或無法回覆。建議對這些困難回覆或無法回覆之修正論文(Revised manuscript)回覆,可能撰寫之範例:

1.The exact mechanism of laser noise is important and is currently under investigation.

2.The exact mechanism of laser noise is important and will be pursued in a separate study.

3.The exact mechanism of laser noise is uncertain and needs to be investigated further.

回覆重大修改評論之撰寫範例

Based on the current-voltage characteristics of the SI layer, it is believed that at high-bias current the applied voltage to the SI layer is in the transition region. Clearly, detailed knowledge pertaining to the transition from the Ohmic to the SCL regime is important and will be pursued in a separate study. Nevertheless, dc leakage current can be reduced by increasing the thickness of the SI layer and by decreasing the area of the SI layer to which voltage is applied. This leads to the observed improvement in the modulation bandwidth.(1987 APL, Reference 3)

參考文獻(References)

1. W.H. Hsieh, C.N. Liu, Y.C. Huang, C.A. Hsu, S.S. Lei, Y.C. Hsu, Y.C. Tsai, C.H. Lin, C.P. Yu, and W.H. Cheng, "A New Scheme of Oriented Hyperboloid Microlens for Passive Alignment Lasers to Polarization Maintaining Fibers," J Lightwave Technol. 33, Oct. 4187 (2015).

2. P.L. Huang, S.C. Lin, C.Y. Yeh, H.H. Kuo, S.H. Huang, G.R. Lin, L.J Li, C.Y. Su, and W.H. Cheng, " Stable Mode-Locked Fiber Laser Based on CVD Fabrication Graphene Saturable Absorber, " Optics Express, 20, Jan. 24690 (2012).

3. W.H. Cheng, C.B. Su, K.D. Buehring, S.Y. Huang, J. Pooladdej, D. Wolf, D. Perrachione, D. Renner, K.L. Hess, and S.W. Zehr, "High-Speed and High-Power 1.3 μm InGaAsP Buried Crescent Injection lasers with Semi-Insulating Current Blocking Layers," Appl. Phys. Lett., 51, Nov. 1783 (1987).

4. C.J. Fraser, "English Scientific Reports and Presentation" "英文科技論文與會議簡報",方克濤,全華圖書,新北市 (2015).

～簡報結束～

謝謝聆聽

A New Scheme of Oriented Hyperboloid Microlens for Passive Alignment Lasers to Polarization Maintaining Fibers

Wen-Hsuan Hsieh, Chun-Nien Liu, *Student Member, IEEE, Student Member, OSA*, Yi-Chung Huang, *Member, IEEE, Member, OSA*, Cheng-An Hsu, Shih-Chin Lei, Yi-Cheng Hsu, Ying-Chien Tsai, Che-Hsin Lin, Chin-Ping Yu, and Wood-Hi Cheng, *Fellow, IEEE, Fellow, OSA*

摘要: 1.目的、2.方法、3 結果、4 結論、5 結論建議或貢獻度

***Abstract*—[1]A new scheme of oriented-hyperboloid microlens (OHM) with passive alignment to achieve high polarized extinction ratio (PER) is proposed and demonstrated high efficiency coupling of high-power 980 nm pump lasers to polarization maintaining fibers (PMFs). [2]Using an automatic grinding machine and a charge-coupled-device to precisely control and attain the required minor radius of curvature 4–4.8 μm, offset within 0.7 μm, and axis orientation accuracy ±1°, [3]the OHM exhibited a high-average PER of 31.7 dB, and a high-average coupling efficiency of 83.4%. For a 30 dB PER, the angular misalignment tolerance of the OHM was measured to be ±2°. [4]The unique advantage of the proposed OHM is passive alignment to achieve high PER by only aligning the OHM endface of the fast axis parallel to the axis of laser polarization. [5]This newly developed OHM with unique passive alignment to achieve high polarization is beneficial for the applications of laser/PMF modules where mode polarization and high coupling efficiency are required for use in high precision fiber optic gyroscopes as well as many low-cost and high-performance lightwave interconnection applications.**

***Index Terms*—Passive alignment polarization-maintaining fiber, oriented hyperboloid microlens, fiber optic gyroscope.**

導論:1.研究動機, 2.文獻回顧, 3.提 出研究方法, 4.研究目的, 5.預期目標, 6.論文組織架構

I. Introduction

P[1]OLARIZATION maintaining fibers (PMFs) with a double refractive index are single-mode fibers which exhibit good maintenance of linearly polarized light [1]. [1]The PMFs are used in special applications required for preserving polarization properties, such as fiber optic sensing, interferometry, and high- standard lightwave interconnection applications. [1]They are also commonly used in fiber optic gyroscopes for the connection be- tween a high-power 980 nm pump lasers coupled to a modulator via PMFs, since the modulator requires polarized light as input source. [1]The PMFs are called polarization preserving because they allow for the preservation and control of the mode polar- ization state. [1]Therefore, an accurate alignment between pump lasers and PMFs to achieve high coupling efficiency is important to the development of high-performance pump laser modules.

[2]To achieve a high-coupling pump laser module, a common approach is fabricating the tip of single-mode fiber (SMF) as an asymmetric microlens for direct coupling. [2]Several asymmetric microlens structures for coupling to high-power 980 nm pump laser diodes have been demonstrated, such as up-tapered wedge- shaped fibers [2], asymmetric hyperbolic fiber microlenses [3]– [5], anamorphic lenses [6], wedge-shaped fibers [7]–[9], QPSM [10], CWSM [11], AECSM [12], DVCM [13], and HM [14]. [3]Despite numerous studies of fiber microlenses for efficient cou- pling [2]–[14], only limited information is available regarding the accurate positioning necessary for controlling the state of mode polarization for PMFs used in high-performance laser modules.

[4]In this study, a new scheme of oriented-hyperboloid-microlens (OHM) employing automatic grinding and accurate positioning to achieve both high-average coupling and polar- ized extinction ratio (PER) for high-power 980 nm pump lasers coupled to PMFs is proposed. The PMF exhibits the circular stress-applying parts (SAP) and is often referred to as the panda fiber, as shown in Fig. 1. [3]Using an automatic grinding machine and a charge-coupled-device (CCD) to precisely control and at tain the required minor radius of curvature, small offset, and axis orientation, the OHMs can achieve both high-average coupling efficiency and PER. [5]The advantage of orientation-dependent OHMs is that the OHM endface of the fast axis can be visu ally observed and then passively aligned to the axis of the laser polarization direction. [5]This is in contrast to other conventional lasers coupled to PMFs [3], which may require complicated and active alignment to control the state of mode polarization. [5]This study demonstrates that the unique OHM structure employing automatic grinding and accurate positioning techniques enables passive alignment to achieve high PER for lasers coupling into PMFs. [5]Therefore, the proposed OHM may be suitable for use

Manuscript received May 15, 2015; revised July 31, 2015; accepted August 9, 2015. Date of publication August 11, 2015; date of current version September 12, 2015. This work was supported in part by the Ministry of Science and Technology of Taiwan under the contracts MOST 103-2221-E-110-003, MOST 103-2221-E-020-017, NSC 102-2221-E-230-005, and the MOE Program of the Aim for the Top University.

W.-H. Hsieh, C.-N. Liu, and C.-P. Yu are with the Department of Photonics, National Sun Yat-sen University, Kaohsiung 804, Taiwan (e-mail: j180502@hotmail.com; terbovine@gmail.com; cpyu@faculty.nsysu.edu.tw).

Y.-C. Huang is with the CEO Office, Brogent Technologies, Inc., Kaohsiung 806, Taiwan (e-mail: oris.huang@gmail.com).

C.-A. Hsu and Y.-C. Tsai are with the Department of Mechanical Engineering, Cheng-Shiu University, Kaohsiung 833, Taiwan (e-mail: j180502@yahoo.com.tw; yctsai@csu.edu.tw).

S.-C. Lei and C.-H. Lin are with the Department of Mechanical and Electromechanical Engineering, National Sun Uat-sen University, Kaohsiung 804, Taiwan (e-mail: s2004919@gmail.com; chehsin@mail.nsysu.edu.tw).

Y.-C. Hsu is with the Department of Biomechatronics Engineering, National Pingtung University of Science and Technology, Pingtung 912, Taiwan (e-mail: ychsux@mail.npust.edu.tw).

W.-H. Cheng is with the Graduate Institute of Optoelectronic Engineering, National Chung Hsing University, Taichung 402, Taiwan (e-mail: whcheng@mail.nsysu.edu.tw).

Color versions of one or more of the figures in this paper are available online at http://ieeexplore.ieee.org.

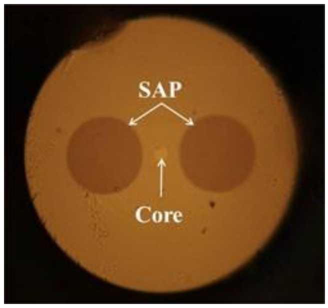

Fig. 1. A cleaved end-face of PMF. The PMF is referred to as a panda fiber with circular SAP.

in high-precision and high-performance fiber-optic gyroscope systems and other lightwave interconnection applications.

[6]The rest of this paper is organized as follows. Section II de- scribes the fabrication of OHMs. The measurements and results are presented in Section III. A discussion and brief summary are given in Section IV.

方式:1. 材料，2. 實驗(架構、步驟、製程)
3. 量測，4. 圖表或 統計分析

II. Fabrication of Oriented Hyperboloid Microlens (OHM)

[1]A single mode 980 nm pump laser from Axcel Photonics [14] was used for the coupling evaluation. [1]The laser diode was coated at the rear facet with a high reflectivity of 95%, and coated at the front facet with an antireflection of 2.5%. These 980 nm high-power lasers typically have far-field divergence angles of 7° (horizontal) × 26° (vertical), with the relative beam waist radius of 3 and 0.8 μm, respectively. The far-field divergence angle was specified as a full angle at the $1/e^2$ maximum of the far-field intensity distribution. [2]The 980 nm laser-to-fiber coupling model was based on the diffraction theory [5], [15]. From the lasers to the OHM, the Fresnel diffraction theory was used for beam propagation through free space. At the lens tip, a phase delay caused by the OHM was added to the laser mode field. In this paper, the ideal curvature radii of $\boldsymbol{R_x}$ in fast axis and $\boldsymbol{R_y}$ in slow axis were designed to be 50.6 and 4.14 μm, respectively. [2]Based on Preston's equation [16], the material removal rate of the fiber tip was proportional to the grinding pressure and the relative velocity between a fiber and a grinding film. Therefore, the material removed from the fiber tip increased as the grinding pressure applied on the fiber increased while the other param- eters were kept constant. [2]As shown in Fig. 2, the fiber grinder employed to fabricate the OHM was designed as a three axis grinding machine and a CCD alignment system. The grinding pressure, the relative position over the axial, and radial axes were controlled by the motorized linear vertical stage **H** with an accuracy of ±10 nm, the motorized cylinders with accuracy $\boldsymbol{\theta}$ of 0.058°, and the servo motor with accuracy $\boldsymbol{\Phi}$ of 0.036°, respectively. These three tolerances were electrically and independently programmed for control, and the fabrication process was fully automated after the initial setting. In addition, a CCD alignment was used to position the PMF relative to its SAP such that the OHM was orientation-dependent.

[1]The PMFs adopted in this study were Fujikura SM98-PS-U25A, as shown in Fig. 1. The mode-field diameter and core-cladding concentricity error were 6.6 and 0.7 μm, respectively.

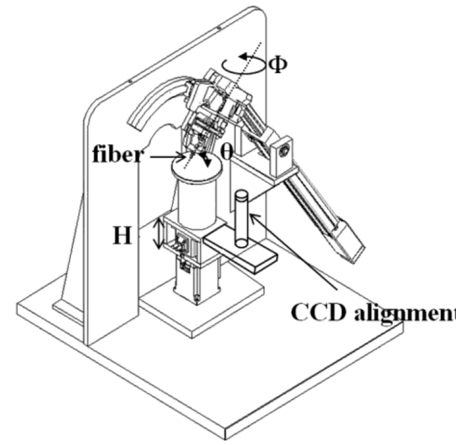

Fig. 2. Schematic diagram of controlled variables of servo motor **(Φ)**, motorized cylinders **(θ)**, vertical stage **(H)**, and CCD alignment.

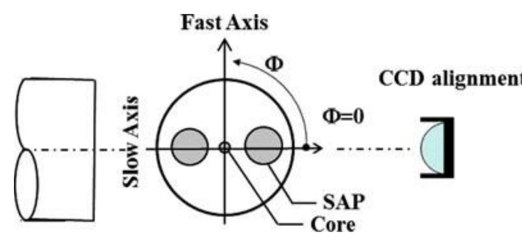

Fig. 3. Schematic diagram of PMF by CCD alignment.

The polarization crosstalk was 30 dB/100m. [2]The OHM was fabricated by grinding a cleaved fiber in a single step. The highest and lowest positions of **H** were controlled to produce two maximum and two minimum grinding pressures while $\boldsymbol{\theta}$ was kept constant at 45°. First, we positioned the core and SAPs of PMF in alignment at $\boldsymbol{\Phi}$ = 0° (slow axis) by CCD, as shown in Fig. 3. After grinding, the long (fast) and short (slow) axes of the approximated elliptical cone were formed at $\boldsymbol{\Phi}$ = 0° and 90°, respectively, as shown in Fig. 4. In order to fabricate an OHM shape, it is necessary to vary the height of **H** (and therefore applied pressure) until the endface was gradually ground sharp, as shown in Fig. 5(a)–(f). [4]After this single-step grinding fabrication, the radius of curvature, offset of OHMs, and orientation accuracy of the microlens were measured at between 3.4–3.5 μm, 0.1–0.7 μm, and ±1°, respectively. After the grinding process, the surface of the OHMs were still rough. A slight arc fusion process was applied to reshape and smoothen the fabricated OHM surface.

[3]A fiber fusion machine, Fujikura 40S, was employed to con trolthe electrode probe and to form the microlens on the fiber tip, as shown in Fig. 6. The electrode arc fused the fiber tip and increased the radius of curvature of OHM. By employing a fine fusing process, the minor radius of curvature was well controlled within 4–4.8 μm which was close to the ideal shape. [3]The OHM samples in this work meet high-average coupling efficiency, correlated to an offset less than 0.7 μm and a small radius of curvature ranging from 4–4.8 μm. The fiber was ground and fused to form the slow axis, fast axis, and endface of the OHM, as shown in Fig. 7(a)–(c), respectively.

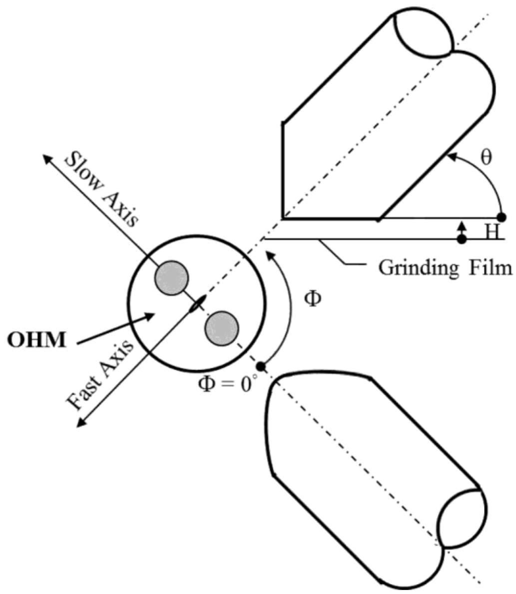

Fig. 4. Fabrication process of OHM.

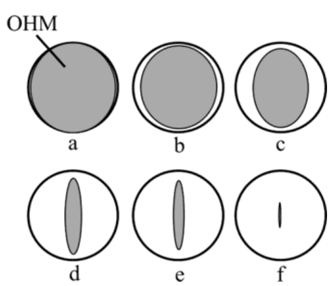

Fig 5. Gradual grinding process in fabrication of OHM.

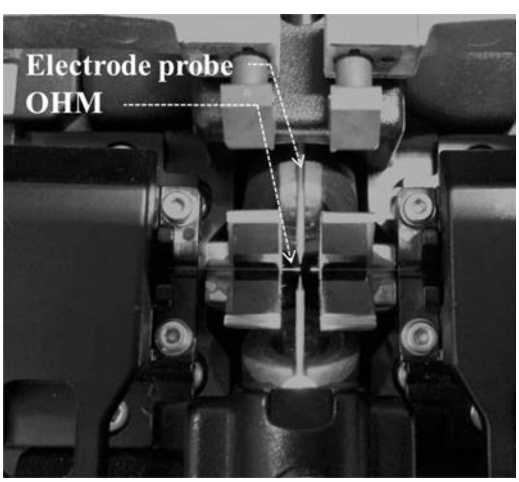

Fig. 6. Fusing process in fiber fusion machine.

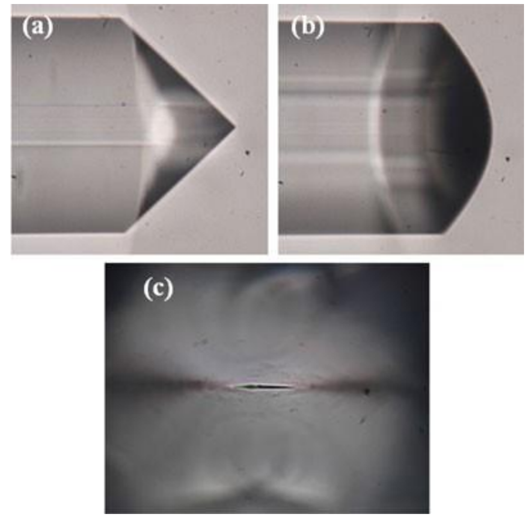

Fig. 7. Optical photons of OHM after grinding and fusion processes in (a) fast axis, (b) slow axis, and (c) endface.

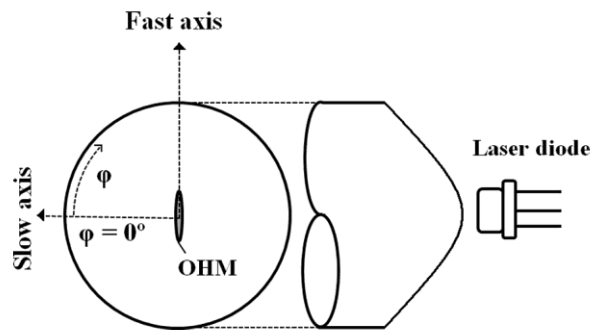

Fig. 8. Schematic setup of PER measurement.

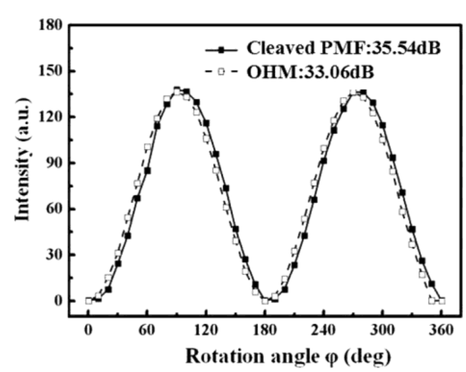

Fig. 9. Linearly polarized distribution of OHM and cleaved PMF.

結果:1.主要結果,2.次要結果,3.圖表分析結果, 4.統計分析結果

III. Measurements and Results

Thirty OHMs were fabricated by single-step grinding and a fine fusing process. The radius of curvature and offset of these samples were measured between 4–4.8 μm and 0.1–0.7 μm, respectively. In order to characterize the quality of their polarized beam, their PER was measured. A high-power 980 nm pump laser diode was connected to an output collimator and laser light was passed through via the OHM into the PMF. The output power of the PMF through a polarizer was then measured by a power-meter and the polarized distribution was obtained. [4]We defined the slow axis of PMF as $\phi = 0^{\circ}$ and measured output power at each 10° from 0° to 360° clockwise, as shown in Fig. 8. For comparison, a cleaved-end PMF was produced in the same experimental structure and similarly measured. [4]Fig. 9 shows the

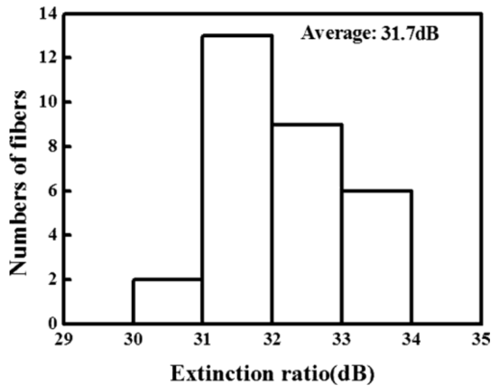

Fig. 10. Histogram of thirty measured PERs of the OHMs.

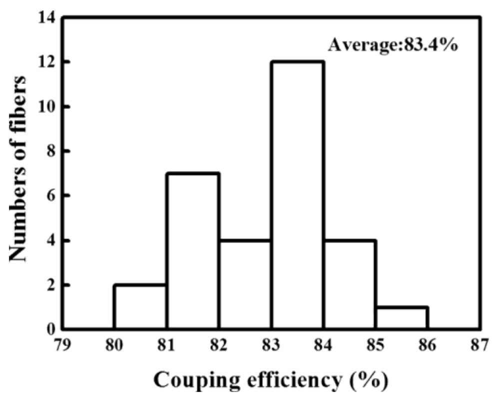

Fig. 11. Histogram of thirty measured coupling efficiencies of the OHMs.

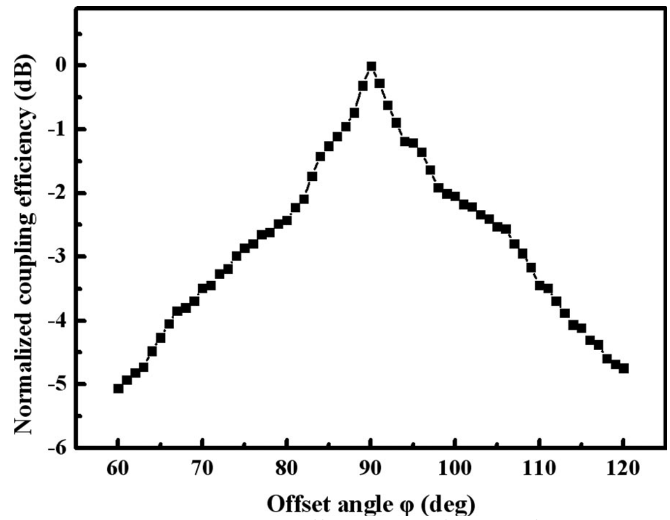

Fig. 12. Normalized coupling efficiency as a function of angular misalignment.

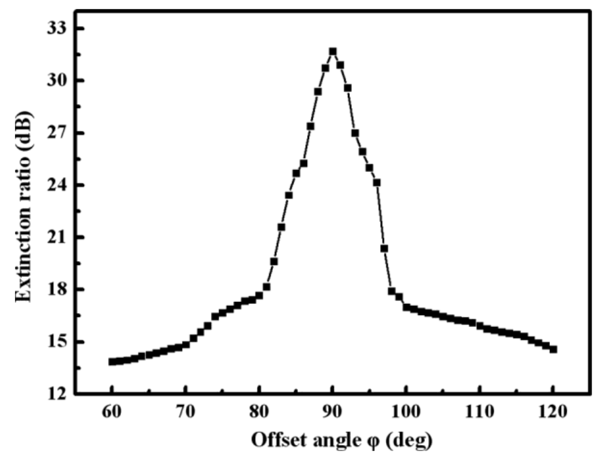

Fig. 13. Measured PER as a function of angular misalignment.

linearly polarized distribution of light through both the OHM-PMF and the cleaved end PMF. The PERs were calculated at about 35.54 and 33.06 dB for the cleaved PMF and OHM-PMF, respectively, from the highest/lowest output power according to 10*log (P_H /P_L) and realized standard linearly polarized distribution. The PER of OHM was smaller than the cleaved PMF. Owing to the stress and thermal effects during the OHM fabrication process, the SAP structure was slightly changed.

[3]A histogram of measured PERs for a total number of 30 OHM samples is shown in Fig. 10. [1]The best value for measured PER was 33.6 dB, and the average PER was 31.7 dB. This result shows that the proposed OHMs maintain good transmission quality for linearly polarized light. [3]Fig. 11 shows a histogram of measured coupling efficiencies from the 980 nm laser diodes into the OHMs for a total of 30 measurements. [1]The best value and average of measured coupling efficiency were 85% and 83.4%, respectively. The result indicates that the OHMs are suitable for use in high-performance pump laser modules.

In a laser module, the misalignment tolerance of the OHMs affected the coupling efficiency and polarization-maintaining characteristic between laser diodes and PMFs. In order to characterize the misalignment tolerance of the OHMs, we defined the slow axis of PMF as $\phi = 0^\circ$ and measured output power for each 1° from 60° to 120°. [3]Fig. 12 shows the normalized coupling efficiencies as a function of the angular misalignment tolerance from laser into the OHM. [4]The –3 dB coupling of the angular misalignment tolerance was measured at ±16° in the fast axis. [3]Fig. 13 shows the PER as a function of the angular misalignment tolerance. The measured 30 dB angular tolerance of the OHM was ±2° in the fast axis. The measured angular misalignment tolerance of a 30 dB PER was more sensitive than the 3 dB coupling, *as* indicated in Fig. 12. From Fig. 13, it was clear that the axis orientation misalignment tolerance was ±2° for a 30 dB PER. [1]The fabricated accuracy of the axis orientation of OHM was ±1° in Fig. 2, which *was* less than the alignment requirement of ±2° necessary to achieve a high PER of 30 dB in Fig. 13. This indicates that the OHM endface of the fast axis can be visually observed and then passively aligned to the axis of the laser polarization direction. The 30 dB PER was easily achieved for high polarization between laser and the PMF by employing OHM. Therefore, the unique advantage of the orientation-dependent OHM is passive alignment to achieve high PER. [1]This study uses automatic grinding and accurate positioning to precisely and quantitatively control the required minor radius of curvature and axis orientation, so that the OHMs can achieve high-average PER and high-average coupling. The high PER and high coupling attained by the proposed OHMs greatly improve potential applications in high- precision fiber optic gyroscopes as well as inertial navigation systems of guided missiles and navigational applications.

討論:1. 結果概述, 2.推論, 3.限制, 4.建議新的研究題目

結論:1. 陳述最重要的研究結果,2. 指出結論的貢獻度

IV. Discussion and Conclusion

[1]In summary, a novel OHM employing automatic grinding and CCD accurate positioning for passive alignment, which can achieve high PER and efficient coupling of high-power 980 nm pump lasers into PMFs, has been proposed and demonstrated. [1]Results showed that the OHMs enabled precisely control and attain the required minor radius of curvature at 4–4.8 μm, offset within 0.7 μm, and axis orientation ±1°, for achieving a high- average coupling efficiency of 83.4% and a high-average PER of 31.7 dB from lasers coupling into PMFs. [1]The fabricated axis orientation accuracy of the OHM was ±1°, which was less than the alignment tolerance of ±2° required to achieve a high PER of 30 dB. [2]This indicates that the OHM endface of the fast axis can be visually observed and passively aligned to the axis of the laser polarization direction. [1]The unique advantage of OHM is that OHM can be easily used for passive alignment to achieve high polarization of laser. This is in contrast to other conventional lasers coupled to PMFs, which may require complicated and active alignment to control the state of mode polarization. [4]In addition, the proposed OHM can be also applied to other types of laser diodes, such as high-power 1480 nm laser diode, by suitable designing of the minor radius of curvature of the OHM to match the laser mode.

[4]The practical packaging of the OHM is based on the butterfly- type laser module in reference [17]. Before the gripper clamping the OHM fiber ferrule, the ferrule should be adjusted such that the fast axis of the OHM, as shown in Fig. 3, is in the hori- zontal direction. All the other packaging procedures are similar to that of the butterfly-type laser modules [17]. [4]This novel design, fully automatic fabrication, and excellent performance of the OHM makes the proposed OHMs potentially attractive for uses in high precision fiber optic gyroscopes as well as many high-performance and low-cost lightwave interconnection applications.

參考文獻

References

[1] J. Noda, K. Okamoto, and Y. Sasaki, "Polarization-maintaining fibers and their applications," *J. Lightw. Technol.*, vol. 4, no. 8, pp. 1071–1089, Aug. 1986.

[2] V. S. Shah, L. Curtis, R. S. Vodhanel, D. P. Bour, and W. C. Yang, "Efficient power coupling from a 980-nm, broad-area laser to a single-mode fiber using a wedge-shaped fiber endface," *J. Lightw. Technol.*, vol. 8, no. 9, pp. 1313–1318, Sep. 1990.

[3] H. M. Presby and C. A. Edwards, "Efficient coupling of polarization-maintaining fibers to laser diodes," *IEEE Photon. Technol.*, vol. 4, no. 8, pp. 897–899, Aug. 1992.

[4] H. M. Presby and C. R. Giles, "Asymmetric fiber microlenses for efficient coupling to elliptical laser beams," *IEEE Photon. Technol.*, vol. 5, no. 2, pp. 184–186, Feb. 1993.

[5] C. A. Edwards, H. M. Presby, and C. Dragone, "Ideal microlens for laser to fiber coupling," *J. Lightw. Technol.*, vol. 11, no. 2, pp. 252–257, Feb. 1993.

[6] R. A. Modavis and T. W. Webb, "Anamorphic microlens for laser diode to single-mode fiber coupling," *IEEE Photon. Technol.*, vol. 7, no. 7, pp. 798–800, Jul. 1995.

[7] H. Yoda and K. Shiraishi, "A new scheme of lensed fiber employ- ing a wedge-shaped graded-index fiber tip for the coupling between high-power laser diodes and single-mode fiber," *J. Lightw. Technol.*, vol. 19, no. 12, pp. 1910–1917, Dec. 2001.

[8] H. Yoda and K. Shiraishi, "Cascaded GI-fiber chips with a wedge-shaped end for the coupling between an SMF and a high-power LD with large astigmatism," *J. Lightw. Technol.*, vol. 20, no. 8, pp. 1545–1548, Aug. 2002.

[9] Y. Irie, J. Miyokawa, A. Mugino, and T. Shimizu, "Over 200 mW 980 nm pump laser diode module using optimized high-coupling lensed fiber," in *Proc. Opt. Fiber Commun. /Int. Conf. Integrated Optics Opt. Fiber Commun. Conf.*, San Diego, CA, USA, Feb. 1999, pp. 238–240.

[10] S. M. Yeh, Y. K. Lu, S. Y. Huang, H. H. Lin, C. H. Hsieh, and W. H. Cheng, "A novel scheme of lensed fiber employing a quadrangular-pyramid-shaped fiber endface for coupling between high-power laser diodes and single-mode fibers," *J. Lightw. Technol.*, vol. 22, no. 5, pp. 1374–1379, May 2004.

[11] S. M. Yeh, S. Y. Huang, and W.-H. Cheng, "A new scheme of conical-wedge-shaped fiber endface for coupling between high-power laser diodes and single-mode fibers," *J. Lightw. Technol.*, vol. 23, no. 4, pp. 1781–1786, Apr. 2005.

[12] Y. K. Lu, Y. C. Tsai, Y. D. Liu, S. M. Yeh, C. C. Lin, and W. H. Cheng, "Asymmetric elliptic-cone-shaped microlens for efficient coupling to high-power laser diodes," *Opt. Exp.*, vol. 15, pp. 1434–1442, 2007.

[13] Y. D. Liu, Y. K. Lu, Y. C. Tsai, S. M. Yeh, C. C. Lin, and W. H. Cheng, "New scheme of double-variable-curvature microlens for efficient coupling high-power lasers to single-mode fibers," *J. Lightw. Technol.*, vol. 29, no. 6, pp. 898–904, Mar. 2011.

[14] Y. C. Huang, W. H. Hsieh, Y. C. Hsu, M. T. Sheen, Y. S. Lin, J. L. Chen, Y. C. Tsai, and W. H. Cheng, "New scheme of hyperboloid microlens for high-average and high-yield coupling high-power lasers to single-mode fibers," *J. Lightw. Technol.*, vol. 31, no. 11, pp. 1681–1686, Jun. 2013.

[15] Y.-K. Lu, P. Yeh, and W.-H. Cheng, "Direct near-field phase measurement of laser diodes employing a single-mode fiber interferometer," *Opt. Lett.*, vol. 35, pp. 3643–3645, 2010.

[16] J. W. Goodmam, *Introduction to Fourier Optics*. San Francisco, CA, USA: McGraw-Hill, 1968, ch. 4–5.

[17] Y. D. Liu, M. T. Sheen, Y. C. Hsu, H. K. Hsu, Y. C. Tsai, and W. H. Cheng, "Online postweld shift measurement of butterfly-type laser module employing high-resolution capacitance displacement measurement system," *Trans. Electron. Packag. Manuf.*, vol. 33, pp. 91–97, 2010.

Wen-Hsuan Hsieh received the M.S. degree from the Department of Electrical Engineering, National University of Kaohsiung, Kaohsiung, Taiwan, in 2010. He is currently working toward the Ph.D. degree in the Department of National Sun Yat-Sen University, Kaohsiung. His research interests include fabrication and measurement of fiber microlens, near-field measurement of fiber coupling, and the fabrication of 980 nm pump laser module.

Chun-Nien Liu received the B.S. degree in physics from the National Changhua University of Education, Changhua, Taiwan, and the M.S. degree from the De- partment of Photonics, National Sun Yat-sen University, Kaohsiung, Taiwan, in 2010, where he is currently working toward the Ph.D. degree in the Department of Photonics. His research interests include fabrication and applications of rare- earth crystal fiber. He is a Student Member of the Optical Society of America.

Yi-Chung Huang (M'01) received the B.S. and M.S. degrees in electrical en- gineering from National Sun Yat-sen University, Kaohsiung, Taiwan, and the Ph.D. degree from the Institute of Electro-Optical Engineering, National Sun Yat-sen University. He is currently the Chief Engineer in CEO office at Brogent Technologies, Inc., Kaohsiung, Taiwan. From 2001 to 2003, he worked with LightSpeed Technology Corp. on the development of optical transceiver mod- ule and active components for optical communication systems. From 2008 to 2010, he was a Postdoctoral Researcher in the Graduate Institute of Photonics and Optoelectronics, National Taiwan University, Taipei, Taiwan. From 2010 to 2014, he was a Postdoctoral Researcher in the Department of Photonics, Na- tional Sun Yat-sen University, Kaohsiung, Taiwan. His major research interests include broadband Cr-doped fiber, specialty fiber, packaging for optical active components, and high-power LED based on glass host. He is a Member of the Optical Society of America.

Cheng-An Hsu received the M.S. degree from the Department of Mechanical Engineering/Mechatronic Engineering, National Cheng Shiu University, Kaohsiung, Taiwan, in 2014. His research interests include CAD, mechanism design, and mechatronics.

Shih-Chin Lei received the B.S. degree from the Department of Bio-Mechanic Engineering, National Chiayi University, Chiayi, Taiwan, in 2014. He is currently a graduate student in the Department of Mechanical and Electromechanical Engineering, National Sun Yat-sen University, Kaohsiung, Taiwan. His research interests include fabricating lensed optic fibers with advanced micromachining techniques.

Yi-Cheng Hsu was born in Kaohsiung, Taiwan, in 1974. He received the B.S. degree in electromechanical engineering and the Ph.D. degree in electrooptical engineering from National Sun Yat-sen University, Kaohsiung, Taiwan, in 1998 and 2005, respectively. From 2000 to 2001, he was a Module Engineer with Taiwan Semiconductor Manufacturing Company Ltd., Hsinchu, Taiwan. From 2004 to 2006, he was a Postdoctoral fellow at the Institute of Electro-Optical Engineering, National Sun Yat-sen University. He is currently an Associate Professor with the Department of Biomechatronics Engineering, National Pingtung University of Science and Technology, Pingtung, Taiwan. His research interests include the design and fabrication of high performance laser module, laser welding technology for low-cost and high-speed laser module packaging, LED module packaging, laser module packaging, and design and fabrication of fiber sensor.

Ying-Chien Tsai received the B.S. degree from National Cheng Kung University, Tainan, Taiwan, in 1969, and the Ph.D. degree from the Oklahoma State University, Stillwater, OK, USA, in 1982, both in mechanical engineering. He is currently the Chair Professor in the Department of Mechanical Engineering, Cheng-Shiu University, Kaohsiung, Taiwan, as well as an Adjunct Professor in the Department of Mechanical and Electromechanical Engineering, National Sun Yat-sen University, Kaohsiung. His primary research interests include measurement in flip-chip, opto-electronic submodule packaging, and mechanism design. He is a Member of the Chinese Society of Mechanical Engineering, the Chinese Institute of Engineers, the Society of Taiwan Automatic Engineers, the Chinese Society of Mechanism and Machine Theory, and the American Society of Mechanical Engineers.

Che-Hsin Lin received the B.S. degree in chemical engineering from National Taiwan University, Taipei, Taiwan, in 1994 and the M.S. and Ph.D. degrees in biomedical engineering from National Cheng Kung University, Tainan, Taiwan, in 1996 and 2002, respectively. His master study focused on bioceramics and biomechanics. He then worked on MEMS for bioanalytical applications in the Ph.D. He is currently an Associate Professor at the Department of Mechanical and Electro-Mechanical Engineering, National Sun Yat-sen University, Kaohsiung, Taiwan. His research interests include MEMS fabrication technologies, bio-MEMS, microfluidic systems, and applications of atmospheric plasma.

Chin-Ping Yu received the B.S. degree in electrical engineering and the Ph.D. degree in communication engineering from the National Taiwan University, Taipei, Taiwan, in 1997 and 2004, respectively. From 2004 to 2007, he was a Postdoctoral Research Fellow with the Graduate Institute of Electro-Optical Engineering, National Taiwan University. In August 2007, he joined the Faculty of the Department of Photonics, National Sun Yat-sen University, Kaohsiung, Taiwan, where he is currently an Associate Professor. His research interests include numerical methods for solving optical waveguide problems, fabrication of optical fiber sensors, and applications of photonic-crystal structures.

Wood-Hi Cheng (M’95–SM’00–F-09) received the Ph.D. degree in physics from Oklahoma State University, Stillwater, OK, USA, in 1978. From 1994 to 2014, he was a Professor, the Director of the Institute of Electro-Optical Engineering, the Dean of College Engineering, the Director of the Southern Taiwan Opto-Electronics Center of Excellence, and a Chair Professor, all from National Sun Yat-sen University, Kaohsiung, Taiwan.

He is currently a Professor at the Graduate Institute of Optoelectronic Engineering, National Chung Hsing University, Taichung, Taiwan. His research and development has contributed to photonic package technologies, including high-speed laser module packaging, high-coupling devices and modules packaging, mode-locked fiber lasers employing carbon nanotubes and graphene, high-reliability glass-doped white-light-emitting diodes, wideband Ce-doped fibers, and 300-nm ultra broadband Cr-doped fiber amplifiers.

He served as the Chair for the IEEE Photonics Society, Taipei Chapter, from 1999–2000, served as the Chair for the OSA, Taipei Chapter from 2005–2006, and also served as the Program Director of Optoelectronics in the Ministry of Science and Technology (MOST) of Taiwan providing research grants and direction during 2009–2011. He received three-times Outstanding Research Award by the MOST, the IEEE Photonics Engineering Achievement Award in 2010 for his contributions to design, development, and commercialization of compact solid-state laser modules, and the 2011–2013 IEEE Photonics Society Distinguished Lecturer Award for the title of lecturers: The art and science of packaging photonics devices and modules and Broadband chromium-doped fiber amplifiers for next-generation optical communication systems. He is a Fellow of OSA and SPIE.

Stable mode-locked fiber laser based on CVD fabricated graphene saturable absorber

Pi Ling Huang,[1] Shau-Ching Lin,[1] Chao-Yung Yeh,[2] Hsin-Hui Kuo[3], Shr-Hau Huang[1], Gong-Ru Lin,[4] Lain-Jong Li,[5] Ching-Yuan Su,[5] and Wood-Hi Cheng[1,*]

[1]*Department of Photonics, National Sun Yat-sen University, Kaohsiung, Taiwan*

[2]*Metal Industries Research and Development Center, Kaohsiung, Taiwan*

[3]*Department of Electrical Engineering, National University of Kaohsiung, Kaohsiung, Taiwan*

[4]*Graduate Institute of Photonics and Optoelectronics, National Taiwan University, Taipei, Taiwan*

[5]*Research Center for Applied Sciences, Academia Sinica, Taipei 11529, Taiwan*

**whcheng@mail.nsysu.edu.tw*

摘要: 1.目的、2.方法、3 結果、4 結論、5 結論建議或貢獻度

Abstract: **[1]**A stable mode-locked fiber laser (MLFL) employing multi-layer graphene as saturable absorber (SA) is presented. **[2]**The multi-layer graphene were grown by chemical vapor deposition (CVD) on Ni close to A-A stacking. **[3]**Linear absorbance spectrum of multi-layer graphene was observed without absorption peak from 400 to 2000 nm. **[1]**Optical nonlinearities of different atomic-layers (7-, 11-, 14-, and 21- layers) graphene based SA are investigated and compared. **[3]**The results found that the thicker 21-layer graphene based SA exhibited a smaller modulation depth (MD) value of 2.93% due to more available density of states in the band structure of multi-layer graphene and favored SA nonlinearity. **[3]**A stable MLFL of 21-layer graphene based SA showed a pulsewidth of 432.47 fs, a bandwidth of 6.16 nm, and a time-bandwidth product (TBP) of 0.323 at fundamental soliton-like operation. **[5]**This study demonstrates that the atomic-layer structure of graphene from CVD process may provide a reliable graphene based SA for stable soliton-like pulse formation of the MLFL.

OCIS codes: (140.4050) Mode-locked lasers; (060.4370) Nonlinear optics, fibers.

References and links

1. F. Dausinger, F. Lichtner, H. Lubatschowski, "Femtosecond Technology for Technical and Medical Applications", Springer:Berlin., Topics Appl. Phys. 96 (2004).
2. U. Keller,"Recent developments in compact ultrafast lasers", Nature, **424**, 831-838. (2003)
3. H. A. Haus, "Mode-locking of lasers", IEEE J. Sel. Top. Quantum Electron., **6**, 1173–1185 (2000).
4. Z. Sun, T. Hasan, F. Torrisi, D. Popa, G. Privitera, F. Wang, F. Bonaccorso, D. M. Basko, and A. C. Ferrari "Graphene mode-locked ultrafast laser", ACS Nano, **4**, 803–810 (2010).

5. I. Hernandez-Romano, D. Mandridis, D. A. May-Arrioja, J. J. Sanchez-Mondragon, and P. J. Delfyett, “Mode-locked fiber laser using an SU8/SWCNT saturable absorber”, Opt Lett., **36**, 2122–2124 (2011).

6. J. C. Chiu, Y. F. Lan, C. M. Chang, X. Z. Chen, C. Y. Yeh, C. K. Lee, G. R. Lin, J. J. Lin, W. H. Cheng,. “Concentration effect of carbon nanotube based saturable absorber on stabilizing and shortening mode-locked pulse”, Optics Express, **18**, 3592-3600 (2010)

7. Y. Hernandez, V. Nicolosi, M. Lotya, F. M. Blighe, Z. Sun, S. De, I. T. McGovern, B. Holland, M. Byrne, Y. K. Gun'Ko, J. J. Boland, P. Niraj, G. Duesberg, S. Krishnamurthy, R. Goodhue, J. Hutchison, V. Scardaci, A. C. Ferrari and J. N. Coleman,” High-yield production of graphene by liquid-phase exfoliation of graphite”, Nature Nanotechnology, **3**, 563-568 (2008).

8. S. Y. Set, H. Yaguchi, Y. Tanaka, M. Jablonski, Y. Sakakibara, A. Rozhin, M. Tokumoto, H. Kataura, Y. Achiba, and K. Kikuchi, “Mode-locked Fiber Lasers based on a Saturable Absorber Incorporating Carbon Nanotubes,” in Proc. Optical Fiber Communication Conf. ’03, Atlanta, GA, 2003, paper PD44.

9. Q. Bao, H. Zhang, Y. Wang, Z. Ni, Y. Yan, Z. Shen, K. P. Loh, and D. Y. Tang, “Atomic layer graphene as saturable absorber for ultrafast pulsed laser,” Adv. Funct. Mater. **19**, 3077–3083 (2009).

10. H. Zhang, D. Y. Tang, L. M. Zhao, Q. L. Bao and K. P. Loh, “Large energy mode locking of an erbium-doped fiber laser with atomic layer graphene,” Optics Express, **17**, 17630-17635 (2009).

11. H. Zhang, D. Y. Tang, L. M. Zhao, Q. L. Bao and K. P. Loh, “Vector dissipative solitons in graphene mode locked fiber lasers,” Optics Communications, **283**, 3334-3338 (2010).

12. W. D. Tan, C. Y. Su, R. J. Knize, G. Q. Xie, L. J. Li, and D. Y. Tang, “Mode locking of ceramic Nd:yttriu, aluminum garnet with graphene as a saturable absorber,” Appl. Phys. Lett., **96**, 031106-1-031106-3 (2010).

13. F. Bonaccorso, Z. Sun, T. Hasan and A. C. Ferrari, “Graphene photonics and optoelectronics”, Nature Photonics, 4, 611-622 (2010).

14. T. Hasan, Z. Sun, F. Wang, F. Bonaccorso, P. H. Tan, A. G. Rozhin, and A. C. Ferrari, “ Nanotube–polymer composites for ultrafast photonics”, Adv. Mater., 21, 3874–3899 (2009).

15. A. H. C. Neto, F. Guinea, N. M. R. Peres, K. S. Novoselov and A. K. Geim, “The electronic properties of graphene”, Rev. of Modern Phys., **81**, 109–162 (2009).

16. A. Martinez, K. Fuse, B. Xu, and S. Yamashita, “Optical deposition of graphene and carbon nanotubes in a fiber ferrule for passive mode-locked lasing”, Opt. Express **18**, 23054-23061 (2010).

17. U. Keller and A. C. Tropper, “Passively modelocked surface-emitting semiconductor lasers”, Physics Reports, **429**, 67-120 (2006).

18. Nonlinear Optics in semiconductor, **59** (Ed.: E. Garmine), Academic, San Diego, CA 1999.

19. A. H. C. Neto,” Graphene Phonons behaving badly”, Nat. Mater., **6**, 176-177 (2007).

20. A. Reina, X. Jia, J. Ho, D. Nezich, H. Son, V. Bulovic, M. S. Dresselhaus, and J. Kong,” Large area, few-layer graphene films on arbitrary substrates by chemical vapor deposition”, Nano Letters, **9**, 30-35 (2009).

21. C. Y. Su, D. Fu, A. Y. Lu, K. K. Liu, Y. Xu, Z. Y. Juang, and L.-J. Li,” Transfer printing of graphene strip from the graphene grown on copper wires”, Nanotechnology, **22**, 185309-185314 (2011).

22. R. R. Nair, P. Blake, A. N. Grigorenko, K. S. Novoselov, T. J. Booth, T. Stauber, N. M. R. Peres, A. K. Geim, “Fine Structure Constant Defines Visual Transparency of Graphene”, Science, **320**, 1308-1308 (2008).

23. M.A. Pimenta, G. Dresselhaus, M.S. Dresselhaus, L.G. Cancado, A. Jorio and R. Saito, “Studying disorder in graphite-based systems by Raman spectroscopy”, Phys. Chem. Chem. Phys., 2007, 9, 1276–1291

24. A.C. Ferrari, J.C. Meyer, V. Scardaci, C.Casiraghi, M. Lazzeri, F. Mauri, S. Piscanec, D. Jiang, K.S. Novoselov, S. Roth, and A.K. Geim, "Raman Spectrum of Graphene and Graphene Layers", Phy. Rew. Lett., **97**, 187401 (2006).

25. F. Wang, A. G. Rozhin, Z. Sun, V. Scardaci, R. V. Penty, I. H. White and A. C. Ferrari, "Fabrication, Characterization and Mode Locking Application of Single-Walled Carbon Nanotube/Polymer Composite Saturable Absorbers", Int. J. Mater. Form., **1**, 107-112 (2008).

26. M. L. Dennis and I. N. Duling III," Experimental study of sideband generation in femtosecond fiber lasers", IEEE J. Quantum Electron., **30**, 1469-1477 (1994).

導論:1.研究動機, 2.文獻回顧, 3.提 出研究方法, 4.研究目的, 5.預期目標, 6.論文組織架構

1. Introduction

[1]Ultrafast lasers possess several applications, such as optical fiber communications, ultrafast probing, nonlinear microscopy, optical coherent tomography, and frequency comb generation [1-2]. [1]A passively mode-locked erbium-doped fiber laser (MLEDFL) is able to generate pulses ranging from picosecond (ps) to femtosecond (fs). [1]The pulse producing mechanism is initiated from noise filtering by saturable absorber (SA) with nonlinear absorption properties [3]. [1]The SA widely used in passive mode-locked lasers is semiconductor saturable absorber mirror (SESAM). [1]However, the drawbacks of SESAM are cost-ineffective and a time-consuming fabricated process. [2]Recently, single-wall carbon nanotubes (SWCNTs) of 1D and graphene of 2D carbon allotrope have been noticed due to their large optical nonlinearity and low saturation intensity [4-7]. [2]The first passive mode-locked fiber laser (MLFL) based on SWCNT-SA was reported by S. Y. Set et al. in 2003 [8]. [2]Recently, the atomic layer graphene as SA for ultrafast pulsed lasers were also demonstrated by Q. Bao et al. [9-12]. [1]Graphene has excellent optical properties, such as optically visualized, high transparency, and linear absorption. [1]It also has ultra-fast relaxation time and the SA is not limited by band gap because of its point band gap structure. [2]Therefore, graphene can be used as fast SA with wide spectral operated range [13-16]. [3]However, mono-atomic layer graphene have relatively high nonlinearity that makes a laser cavity not easy to form a stable soliton pulse [9]. [3]In our nonlinear optical transmission experiments, we recognized that in addition to saturable absorption, the inverse saturation absorption (ISA) could also be formed at a higher intensity level. [3]The ISA could be caused by two photon absorption (TPA) which was similar to the phenomena reported in the SESAM SA [17]. [3]The ISA from a thinner layer graphene could destroy the stability of mode locked pulse formation. [3]Consequently, a thicker layer of graphene with less nonlinearity was identified as the mode locker to reduce the TPA and suppress the ISA. [2]Furthermore, atomic-layer graphene showed high nonlinear absorption which implied high nonlinear dispersion from Kramers-Kronig relationship. [2]Total dispersion was contributed from all the optical elements in the cavity including linear and nonlinear dispersion [9, 18-19]. [2]The nonlinear dispersion, such as self phase modulation (SPM) was contributed from SMF and high-order dispersion of graphene. [2]The total nonlinear dispersion

inside the laser cavity could be compensated by anomalous linear dispersion from SMF to generate stable soliton pulses [9].

[4]In this study, optical nonlinearities of different atomic-layers (7-, 11-, 14-, and 21- layers) graphene based SA are investigated and compared. [5]It was found that the thicker 21-layer graphene based SA exhibited a small MD value of 2.93%.[5]Compared with the thinner 7-, 11-, and 14- layers, the results showed that a better stable MLFL with the thicker 21-layer graphene based SA exhibited a pulsewidth of 432.47 fs, a bandwidth of 6.16 nm, and a time-bandwidth product (TBP) of 0.323 at fundamental soliton-like operation. [5]This study demonstrates that the atomic-layer structure of graphene from CVD process may provide a reliable graphene based SA for stable soliton-like pulse formation of the MLFL.

方式:1. 材料，2. 實驗(架構、步驟、製程)3. 量測，4. 圖表或 統計分析

2. Methods

[1]Different layers of graphene were produced by using a CVD method [20-21]. [1]For the CVD process of graphene on Ni substrate, the substrate structure of Ni(300 nm)/SiO_2(300 nm)/Si was put on a quartz plate and then loaded into the center of a tubular furnace. [2]The chamber was evacuated to ~5 mTorr and the temperature was increased to 1000^oC during the process. [2]Prior to growth, a pretreatment step was performed under a H_2 atmosphere with 400 sccm flow at 2.8 Torr for 10 minutes. [2]In the growth step, a gas mixture of methane and hydrogen (CH_4 = 80 sccm and H_2 = 40 sccm) was introduced for 10 minutes. [2]The system was then cooled down to room temperature to complete the growth. [2]To transfer the as-grown graphene onto the substrate, the Ni substrate after the CVD growth was coated with a layer of Poly (methyl methacrylate) (PMMA) by spinning-coating method, followed by baking at 90^oC for 1 minute. [2]Then the PMMA-caped Ni substrate was immerged into a diluted HCl solution (HCl/Water = 1:3) for 20 minutes to etch away the Ni thin layer. [2]The PMMA-caped graphene film was floated on the solution surface, and then it was transferred to a deionized (DI) water to dilute and remove the etchant and residues. [2]The PMMA/graphene was transferred to the receiving substrate and dried on a hot-plate. [2]The PMMA was removed by warm acetone (90^oC), and then the sample was rinsed with isopropyl alcohol and DI water. [2]To strip off the graphene film from the quartz substrate, the graphene was covered by an aqueous solution of polyurethane (PVA). [2]After water evaporation, graphene with a supporting layer of PVA film was laminated from the quartz substrate. [2]The composite film of graphene/PVA was then obtained.

[2]Figure 1 shows an all-fiber passive MLFL system. [3]An 85 cm highly doped erbium fiber (LIEKKITM Er80-4/125) was used as the gain medium. [3]It was pumped by a 980 nm diode laser via a wavelength division multiplexer (WDM). [3]The graphene films were inserted between two FC/APC fiber connectors as a SA to generate the mode-lock pulses. [3]An isolator was employed to ensure the unidirectional operation, a polarization controller was utilized to

optimize mode-locking. [3]The emission light from EDF gain passed the graphene films then fed back into ring laser with partial transmission by 40/60 output coupler. [3]The 60% port was connected to a 10/90 coupler for separating the laser output to optical spectrum analyzer, power meter, autocorrelator, oscilloscope, and radio-frequency spectrum analyzer. [4]Figure 2 shows the photos of 7-, 11-, and 14- layers of the graphene samples, the dimension of the quartz substrate are around 15 mm by 15 mm.

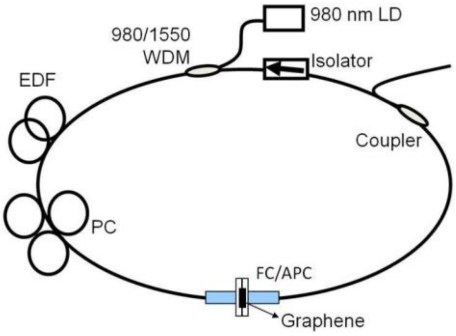

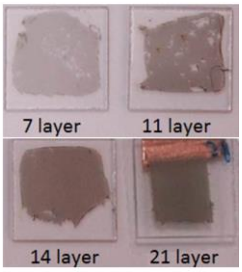

Fig.1. Experimental setup of MLFL ring incorporating graphene SA. Fig. 2. Different layers of the graphene samples

結果:1.主要結果,2.次要結果,3.圖表分析結果, 4.統計分析結果

討論:1. 結果概述, 2.推論, 3.限制, 4.建議新的研究題目

3. Results and discussions

[2]The linear absorption spectra of various layers of graphene were measured and all traces showed featureless from 400 to 1800 nm as theoretically expected [22]. [3]The linear absorption spectrum of the 21-layer graphene was showed in Fig. 3. [3]The CVD-deposited graphene was well-formatted close to A-A stacked structure. [3]Figure 3 (inset) plots the Raman spectrum of graphene-PVA film with two typical Raman peaks G (~1580 cm^{-1}, line width 24 cm^{-1}) and 2D (~2726 cm^{-1}, line width 63 cm^{-1}). The G-band was a doubly degenerate phonon mode at the Brillouin zone (BZ) center that was Raman active for sp^2-hybridized carbon-carbon bonds in graphene. The 2D-band was originated from a double-resonance process of crystalline graphite. The broaden line width of the 2D-band was mainly due to the multi-layer stacks. An increase in the number of defects among graphene would result in an increase of the D-band (~1350 cm^{-1}) intensity. In this case, the D-band was not observed in the Raman spectrum, suggesting a low defect-level of graphene was prepared [23-24].

The nonlinear transmission characteristics were measured using a SWCNT based SA MLFL. The laser was operated at a central wavelength of 1558.88 nm with a repetition rate of 25.51 MHz and pulse duration of 483 fs. Through a broadband attenuator, the laser output was able to provide intensity up to 80 MW/cm^2. A coupler was connected after the attenuator so that the output power levels with and without passing the SAs could be measured simultaneously. The single-pass optical transmission then was derived [25]. [2]The MD of the 7-, 11-, 14- and 21- layers graphene based SA were measured at 3.98%, 3.50%, 3.28% and 2.93%, respectively. [2]The nonsaturable loss of the 7-, 11-, 14- and 21- layers graphene based SA were also measured at 18.40%, 29.50%, 35.14% and 53.05%, respectively. [3]Figure 4 showed the nonlinear transmission characteristics of the 21-layer graphene SA.

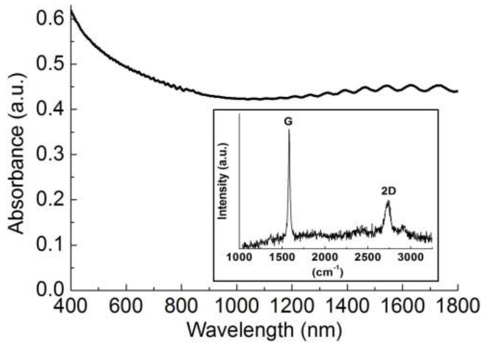

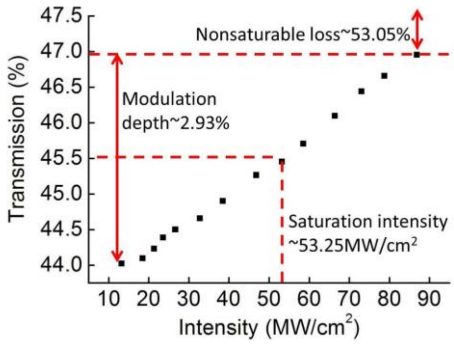

Fig. 3. Linear absorption spectrum and Raman spectrum (inset) with a 473 nm excitation laser of 21-layer graphene on PVA film. Fig. 4. Nonlinear transmission of 21-layer SA.

The performance of MLFL using the 7-, 11-, 14- and 21- layers graphene based SA with different SMF fiber lengths were investigated and compared. The thinner 7-, 11- and 14- layers of graphene based SA were difficult to form a stable soliton-like pulse unless extra SMFs were added. The reason is the thinner layer graphene samples have relatively high MD that makes it difficult for a laser cavity to form a stable soliton pulse and it may need extra SMF to compensate the dispersion. In comparison with the thicker 21-layer graphene as SA, a stable mode locking is easy to form. This may be due to more available density of states in the band structure of stacking-layer graphene than the thinner layer and favored low order nonlinear optics control of graphene inside the cavity. The comparison of passively MLFL performance based on graphene SA is shown in Table I.

[3]Table I. Performance comparison of MLFLs for different layers of graphene SA.

Number of layers	Length of SMF (m)	Pumping current (mA)	Spectra width (nm)	Pulse energy (nJ)	Pulse duration (fs)	Pulse stability
7	5.4+ 50	122	2.20	0.56	1147	Stable
11	5.4+0	108	4.48	0.01	*	Quasi-Stable
11	5.4+10	146	3.11	0.15	715	Stable
14	5.4+0	109	2.86	0.03	*	Quasi-Stable
14	5.4+5	173	3.48	0.07	563	Stable
21	5.4+0	142	6.16	0.05	483	Stable

* Due to the power fluctuation, the autocorrelator was not available to measure the pulsewidth.

[2]For a passive MLFL using a 21-layer graphene as SA; the threshold pump power in continuous wave (cw) lasing was about 33 mW. The mode-locked pulses were self-started as the pumping power increased to 53.30 mW. The optical spectrum of the mode locked pulse is shown in Fig. 5(a). The spectrum was centered at 1559.12 nm with 3 dB spectral bandwidth of 6.16 nm. In Fig. 5(b), the output pulse train of MLEDF exhibited a repetition rate at about 25.51 MHz and the pulse width was measured of 433 fs from the autocorrelator trace. Further increasing the pumping power to 73.78 mW, the harmonic mode locking was observed which could be confirmed by pulse train with a repetition rate about two times of the fundamental mode locking. The TBP was calculated to be 0.323 which was close to the bandwidth limited case. All optical spectra reveal the Kelly sideband indicating that a soliton-like pulse was generated. The laser cavity included 0.85 m of EDF (GVD:-0.02 ps^2/m), 1.35 m of corning flexcor 1060 (GVD:-0.007 ps^2/m), and 5.4 m of SMF28 (GVD:-0.023 ps^2/m). Based on the Kelly sideband location the total cavity dispersion was estimated to be 0.2124 ps/nm [26].

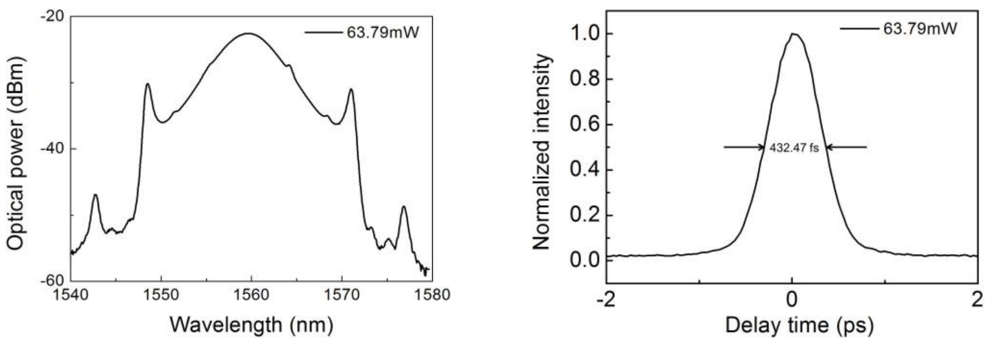

(a)

(b)

Fig. 5 (a) Optical spectrum of the mode-locked laser and (b) Autocorrelator trace.

The RF spectrum of ML pulses was measured by connecting a high sensitivity photo detector to a RF spectrum analyzer (HP8563E). As shown in Fig. 6, the major peak was the cavity repetition rate of 25.67 MHz with a signal-to-noise ratio of 31 dB. In this work, the stability measurement was similar to the previous graphene-based works [9-10], the power stability performance was monitored for 8 hours a day and repeated measurements after 12 hours for two weeks within 2% variation.

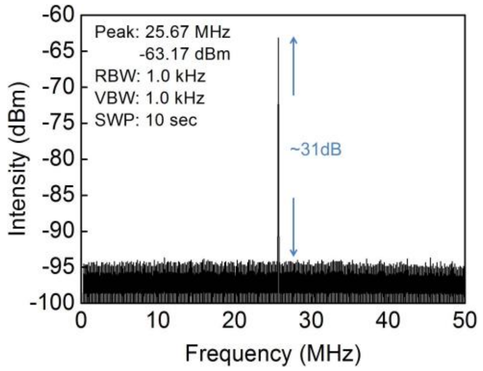

Fig. 6. RF spectrum of fundamental mode-locked laser

[1]The soliton pulse laser performance of fundamental mode locking with 21-layer graphene based SA was shown in Table II. [3]Table II indicated that the stable soliton-like operation was achieved at a pumping level from 53.30 to 63.79 mW. Second-order harmonic soliton-like was achieved at a higher pumping level from 73.78 to 83.26 mW.

[3]Table II. Performance of 21-layer graphene based SA in MLFL.

Pump power (mW)	Pulse duration (fs)	Laser wavelength (nm)	Spectra width (nm)	Pulse energy (nJ)	TBP
53.30	563.64	1559.44	4.64	0.05	0.323
55.80	523.38	1559.28	5.08	0.06	0.328
58.80	483.12	1559.20	5.52	0.07	0.329
61.29	442.86	1559.28	5.92	0.07	0.323
63.79	432.47	1559.12	6.16	0.09	0.329

結論:1. 陳述最重要的研究結果,2. 指出結論的貢獻度

4. Conclusion

[1]In summary, the 7-, 11-, 14- and 21- layers graphene based SA with different SMF fiber lengths for the generation of ultrafast laser pulse were comprehensively studied and compared. [2]It was found that the thinner 7-, 11- and 14- layers of graphene based SA had difficulty in forming a stable soliton-like pulse unless extra SMFs were added. [2]The reason was the thinner layer graphene samples exhibited relatively high MD with ISA made it difficult for a laser cavity to form a stable soliton pulse and needed additional length of SMF to compensate the dispersion. [1]In comparison with the thicker 21-layer graphene as SA, a stable mode locking pulse train was easier to establish. [2]This might be due to more available density of states in the band structure of stacking-layer graphene than the thinner layer and favored nonlinear optics control of graphene inside the laser cavity.

[1]The results showed that the optical nonlinearity of the thick 21-layer graphene based SA exhibited a smaller MD value of 2.93% and a higher saturation intensity of 53.25 MW/cm^2. A stable MLFL of 21-layer graphene based SA showed a pulsewidth of 432.47 fs, a bandwidth of 6.16 nm, and a TBP of 0.323 at fundamental soliton-like operation. [2]This study

demonstrated that the atomic-layer structure of graphene from a CVD process provided a reliable graphene based SA for stable soliton-like pulse formation of the MLFL.